Circulation of Superfluid Suction Vortex

Circulation of Superfluid Suction Vortex

Naoki Kakimoto, Ken Obara, Hideo Yano, Osamu Ishikawa

Circulation of Superfluid Suction Vortex

Naoki Kakimoto[1], Ken Obara[1,2*], Hideo Yano[1,2] and Osamu Ishikawa[1,2]

[1*]Graduate School of Science, Osaka City University, 3-3-138 Sugimoto, Sumiyoshi-ku, Osaka, 558-8585, Osaka, Japan.
[2*]Nambu Institute of Theoretical and Experimental Physics, Osaka City University, 3-3-138 Sugimoto, Sumiyoshi-ku, Osaka, 558-8585, Osaka, Japan.

*Corresponding author(s). E-mail(s): k-obara@osaka-cu.ac.jp;

Abstract

Although the suction vortex is the one of the most common vortices, its flow structure has not been fully understood. The main reasons for this are the experimental difficulty due to the very rapid flow change near the core. However, superfluid helium may help us better understand the suction vortex, because the flow in the superfluid helium can be characterized by the circulation measured by the first sound velocity, and the configuration of the quantized vortex lines can be measured with the second sound attenuation technique, as reported in our previous results [Phys. Rev. Fluids, **6**, 064802 (2021)]. In this paper, we report the effectiveness of an ultrasound circulation meter using the correlation-based differential time-of-flight method. Using this technique, the accuracy for measuring the circulation was greatly improved; we found that the circulation was proportional to the rotation speed of the turbine, which can be interpreted by considering the transport and dissipation of total angular momentum in the fluid.

Keywords: Superfluid ^{4}He, Suction Vortex, Rotating Fluids , Hyrodynamics

1 Introduction

In a classical fluid, vortices can be classified into two types: forced vortices and free vortices. The forced vortices are the vortices that are maintained by

a continuous supply of energy or external torque, and the flow around their axis of symmetry are rotational with constant vorticity. Vorticity is defined as $\boldsymbol{\omega} = \text{rot}\,\boldsymbol{v}$, where $\boldsymbol{v}$ is the velocity field. Currently, vortices with vorticity are fairly well understood. However, the free vortices, on the other hands are not as well understood. The ideal free vortices are the vortices that require neither continuous supply of energy nor external torque. Fluid element rotates due to conservation of angular momentum, and the flow around their axis of symmetry are irrotational. In an ideal free vortex, the azimuthal velocity at the radial position r far enough from its the axis can be written as

$$v_\theta^{(\text{ideal})}(r) = \Gamma/2\pi r, \tag{1}$$

where Γ is the circulation. However, $v_\theta^{(\text{ideal})}(r)$, and therefore the kinetic energy density, rapidly increases as it approaches the axis of rotation. In reality, to avoid forming such a highly kinetic energy region, these vortices tend to form a thin region of non-zero vorticity at the center of rotation, which is called the core of the vortex. In this context, even in a free vortex, the irrotational flow exists only outside the narrow region around the axis of rotation.

In viscous fluid, the vorticity equation tells us that the vorticity should diffuse due to the viscosity, so an additional mechanism is needed for the vortex to be formed permanently. A few theoretical models have been proposed to form such vortices by introducing an inward flow[1]. We are interested in a suction vortex, which is a potential flow around a thin core with finite vorticity. The suction vortex is a permanent vortex maintained by inward and vertical suction flow[2, 3]. There are only a few experimental reports on the suction vortex. The most prominent work on the suction vortex in a water-filled container was reported by Andersen et al.[4, 5]. They showed two distinct regions in the suction vortex other than the boundary layer near the wall: one is the potential flow region and the other is the core-like region where the azimuthal velocity starts to deviate from Eq. (1) Moreover, the surface deformation $\Delta h(r)$ of the fully developed suction vortex shows the following $1/r^2$ dependence:

$$\Delta h(r) = -\frac{1}{2g}\left(\frac{\Gamma}{2\pi r}\right)^2, \tag{2}$$

where $\Delta h(r)$ is the vertical deviation of the liquid position from the liquid at rest. Surprisingly, even today, what we know about the suction vortex is not much more than the two points mentioned above. The main reasons for this is the lack of a technique to directly measure the vorticity.

Our ultimate goal is to understand the structure of the suction vortex using superfluid helium, because all the circulating flow in the superfluid helium can be characterized by the configuration and the motion of the quantized vortex lines[6], and the vortex line density can be measured by the second sound attenuation technique[7, 8]. In this paper, we report a new experimental procedure to obtain the macroscopic circulation of the superfluid suction vortex using an

ultrasound circulation meter (USCM) system with an update of the acquisition technique we reported in Ref. [8]. Further, we evaluated the accuracy of the new procedure by comparing the result with the macroscopic circulation measured by optical surface deformation imaging (OpSDI).

2 Experiments

To agitate superfluid helium in a cylinder, a six-blade Rushton turbine was rotated by a cryogenic motor mounted in the inner chamber, as shown in Fig. 1 (a). When the motor rotated, the inner chamber acted as a centrifugal pump, which caused the rotating flow in the chamber to eject fluid from the slit and force it to return through the drain hole (5 mm), producing a circulating loop. The fluid ejected from the side slit had a non-zero angular momentum as a result of the vorticity generated by the rotating flow in the cylinder. Details are shown in our previous paper[7, 9].
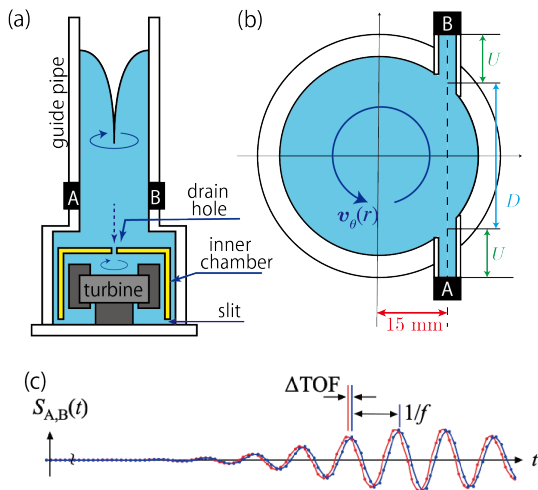

Fig. 1 (a) Side view of cell. A and B indicate the positions of ultrasonic transducers. (b) Schematic (top) view of the circulation meter. (c) Expected waveforms at the receivers, where red points represent $S_B(t)$, the with-flow direction that was detected by transducer B, and blue points represent $S_A(t)$, the against-flow direction that was detected by transducer A. The points are connected by solid curves as a visual guide.

An ultrasonic flowmeter, in general, is commonly used for flow measurement in industrial systems, such as fuel pipelines, and for water- or gas-flow monitoring[10]. A conventional ultrasonic flow meter measures the velocity along the path of an emitted beam of ultrasound; the velocity is determine as the difference in measured time-of-flight (TOF) between the pulses propagating with and against the direction of the flow in the pipe. The principle of our USCM is almost the same as the conventional one, but we measure the difference in TOF between two ultrasonic pulses propagating with and against

the direction of the circulating flow in a horizontal plane. The mathematical formulations are shown in the Appendix of Ref. [8]. In the previous study, the experimental accuracy of TOF measurements was not sufficient because we used a digital storage oscilloscope, and all waveforms were manually obtained and the TOF were manually determined at the rising edge of the envelope of the waveforms. Therefore, the total number of samples were not sufficient because of limitations on sample collection time. So we adopted a fully automatic measurement system that was originally designed for ultrasonic gas flow meters. Here we show our new measurement procedure. Figure 1 (b) shows a schematic view of the USCM in the horizontal plane. In this case, the potential flow $v_\theta(r) = \Gamma_z/2\pi r$ is rotating in the counter-clockwise direction. Here we use the notation Γ_z for the macroscopic circulation because, according to our previous work, this circulation can be treated as a macroscopic circulation that is the sum of the horizontal projection for the vorticity of all quantized vortices in the core. At $T = 1.61$ K, the first sound velocity was 234.3 m/s, and the resonance frequency of our transducers was 390 kHz. Using these parameters, the circulation–TOF correspondence was obtained numerically: $\Gamma_z = 60,241(\tau_a - \tau_w)$, where τ_a and τ_w are the TOF of the first sound pulse against and with, respectively, the circulating flow. Hereafter, we write the difference of these TOF values as ΔTOF. The time sequence for ΔTOF measurement was as follows. The first pulse was transmitted from transducer A, which traveled in the with-flow direction. After some small interval, a second pulse was transmitted from transducer B, which traveled in the against-flow direction. The TOFs are only affected by the rotating flow, so the TOF difference was calculated in the region with rotating flow whose length is indicated as D in Figure 1 (b). The length of the non-rotating region is indicated as U. After some interval, TOF measurements were repeated. Figure 1 (c) shows the expected waveforms $S_{A,B}(t)$ that were observed at transducers A and B, respectively. The expected ΔTOF between two pulses was 100 μs. The sampling frequency of the analog-to-digital converter in this system was $f_s = 2$ MHz, which was faster than the ultrasonic frequency but not fast enough for evaluating the difference between two pulses. However, the correlation-based differential TOF detection technique could improve the time resolution. Here, the correlation function is determined as

$$C(\tau) = \sum_{i}^{N} \left\{ S_B(t_i - \tau) \cdot S_A(t_i) \right\}, \tag{3}$$

where N is the total number of samples in the measurement window, i is the sample index, and $t_i = i/(Nf_s)$ are the sampling times. ΔTOF can be obtained from τ, which gives the maximum of the correlation function. This procedure make it possible to obtain the time resolution for ΔTOF detection much higher than $1/f_s$. One data set of ΔTOF was obtained every 200 ms over 1 minute. Pulse pattern generation, analog-to-digital conversion, and ΔTOF

calculation were all carried out on a microcomputer, and ΔTOF datasets were downloaded to a personal computer.

3 Results and Discussion

Figure 2 (a) shows a typical form of the correlation function as a function of the delay time τ. Several consecutive peaks were observed; the smallest delay time corresponds to ΔTOF, and the interval between the peaks corresponds to the frequency of the first sound. Figure 2 (b) shows the results for the macroscopic circulation of superfluid suction vortex at 1.61 K. Black dots show ΔTOF (left axis) and the calculated circulation Γ_z (right axis). The corresponding errors were less than 0.5%. We also obtained the circulation by means of OpSDI using Eq. (2) to evaluate the validity and accuracy of the USCM with a correlation-based differential TOF method, which is shown by the open squares in the Figure 2 (b). Although we did not measure the surface deformation at 1.61 K
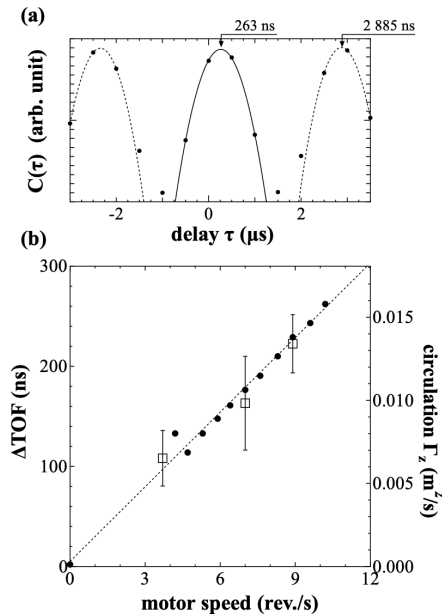

Fig. 2 (a) Typical results of correlation function as a function of delay time, at T = 1.61 K, the motor speed was 10.2 rev./s. Solid and dashed line represent the quadratic fitting to obtain the maximum of the correlation function. (b) Circulation of superfluid suction vortex at 1.6 K. Black dots show ΔTOF (left axis) and the calculated macroscopic circulation Γ_z (left axis) for the USCM. The standard error for each point is less than 0.5%. Open squares with error bars show the circulation obtained by optical observation of the surface deformation, OpSDI, measured at 1.9 K.

with OpSDI in this series of measurements, we already confirmed that there was no temperature dependence in a previous experiment[9]. It was found that

the circulations obtained by USCM were in nearly perfect agreement with those obtained by OpSDI, and that the USCM results were more accurate. This is the first observation that shows the validity of the USCM for liquids in general, because no superfluid parameters or properties were used throughout this procedure.

As a result of the significant improvement in experimental accuracy, we found two facts. First, the circulation measured by OpSDI represents the circulating flow in a thin layer very close to the deformed surface; on the contrary, the circulation measured by the USCM represents the circulating flow in the horizontal plane below the apex of the deformed surface. The agreement between these two circulations implies that the circulation does not depend on depth. Second, the circulation was proportional to the rotation speed of the turbine[11]. We propose that this proportionality can roughly be interpreted by a flow and dissipation of the angular momentum in the liquid; the vertical component of the angular momentum of the liquid in the inner chamber L_I is proportional to the vertical component of the angular momentum of the rotating fluid in the suction vortex, L_V . Because the normal and superfluid components near the rotating turbine were fully turbulent, the superfluid component was driven by the mutual friction force. Thus, it is possible to assume that the liquid in the inner chamber rotates as a rigid body. That is,

$$L_I = \int \rho r^2 \Omega dV \propto \Omega, \tag{4}$$

where ρ and Ω correspond to the density of the liquid and rotation speed of the motor, respectively, and the integral was taken only in the inner chamber. In the guide pipe, on the contrary, the depth dependence of the macroscopic circulation was negligible. Using these assumptions, the following equation may hold:

$$L_V = 2\pi\rho \int_0^H dz \int_{R_C}^R rv_\theta(r)rdr \sim \rho \int_0^H dz \int_0^R \Gamma_z rdr \propto \Gamma_z, \tag{5}$$

where R and H correspond to the radius and height of the pipe, respectively. In addition, the contribution of the angular momentum of the liquid in the core, R_C, can be assumed to be negligibly small because the core region was so thin. Eq. (5) shows that the total angular momentum in the guide pipe is proportional to the macroscopic circulation. Finally, the vertical component of the angular momentum in a thin and complicated gap region between the guide pipe and the inner chamber might be dissipated by the wall, but it is natural to assume that the dissipation of the flow of the angular momentum is proportional to the rotation speed of the motor. Thus, the fact that the circulation is proportional to the rotational speed can be explained by the transport and dissipation of the total angular momentum in the fluid.

4 Summary

In this study, we introduced a correlation-based differential TOF technique for a USMC to measure the circulation of a suction vortex. The accuracy for circulation measurement was greatly improved compared with the results of our previous work. Using this new method, the circulation of the superfluid vortex generated by the turbine was found to be proportional to the rotation speed of the turbine, which can be interpreted considering the transport and dissipation of total angular momentum in the fluid.

The second sound attenuation measurements, especially in the setup in which the second sound wave does not pass through the core region, are needed to clarify the structure of the superfluid suction vortex.

References

[1] J.M. Burgers, Adv. Appl. Mech. **1**, 171–199 (1948)

[2] A.H. Shapiro, Nature **196**, 1080 (1962)

[3] M. Sibulkin, J. of Fluid Mech. **14**, 21 (1962)

[4] A. Andersen, T. Bohr, B. Stenum, J.J. Rasmussen, B. Lautrup, Phys. Rev. Lett. **91**, 104,502 (2003)

[5] A. Andersen, T. Bohr, B. Stenum, J.J. Rasmussen, B. Lautrup, J. of Fluid Mech. **556**, 121 (2006)

[6] S. Inui, T. Nakagawa, M. Tsubota, Phys. Rev. B **102**, 224,511 (2020)

[7] I. Matsumura, K. Ohyama, K. Sato, K. Obara, H. Yano, O. Ishikawa, J. of Low Temp. Phys. **196**, 204–210 (2019)

[8] K. Obara, I. Matsumura, N. Tajima, K. Ohyama, H. Yano, O. Ishikawa, Phys. Rev. Fluids **6**, 064,802 (2021)

[9] H. Yano, K. Ohyama, K. Obara, O. Ishikawa, J. of Phys.: Conf. Ser. **969**, 012,002 (2018)

[10] "Ultrasonic Measurement for Process Control. Theory, Technique, Applications", L.C. Lynnworth, ISBN-0-12-460585-0. Academic Press, Inc. (1989)

[11] In Figure 2, the scattering of the data was larger at the smallest rotation speed. We performed several measurements at smaller rotational speeds,

but the TOF values showed a large variation each time. The reason for this is that at rotation speed below 4 rev./s, the liquid may not follow the motion of the turbine because of the large torque ripple of the motor.